Geomorphology 336 (2019) 95–106

Contents lists available at ScienceDirect

Geomorphology

journal homepage: www.elsevier.com/locate/geomorph

Spatial and temporal patterns of suspended sediment transport in nested urban watersheds

John T. Kemper [a,*], Andrew J. Miller [b,c], Claire Welty [c,d]

[a] Department of Geosciences, Colorado State University, Fort Collins, CO 80523, United States of America
[b] Department of Geography and Environmental Systems, University of Maryland Baltimore County, Baltimore, MD 21250, United States of America
[c] Center for Urban Environmental Research and Education, University of Maryland Baltimore County, Baltimore, MD 21250, United States of America
[d] Department of Chemical, Biochemical, and Environmental Engineering, University of Maryland Baltimore County, Baltimore, MD 21250, United States of America

ARTICLE INFO

Article history:
Received 21 December 2018
Received in revised form 14 March 2019
Accepted 15 March 2019
Available online 18 March 2019

Keywords:
Urban geomorphology
Nested watersheds
Sediment yields
Sediment transport
Turbidity
Urban streams

ABSTRACT

Patterns of sediment yield have been widely investigated across a variety of scales, but few of these studies have been carried out in urban watersheds. The design of this study represented a unique opportunity to use high-frequency sensor data to compare sediment yields across spatial and temporal scales in an urbanized watershed. Near real-time turbidity and discharge data were collected continuously for four years at five stream gages over three nested spatial scales in the highly impervious 14.2-km^2 Dead Run watershed, located in Baltimore County, Maryland, USA. Monthly suspended sediment yields varied by over two orders of magnitude across all stations. Two mid-watershed stations on tributaries to the mainstem of Dead Run are located only about 500 m apart and about 500 m upstream of their confluence, yet displayed observable differences in the timing of their highest sediment yields. Average annual suspended sediment yield was higher at the headwater station with older development (78.2 t/km^2/yr) than at the headwater station with more recent development (47.0 t/km^2/yr). Average annual yields increased with watershed size from the headwater stations to the mid-watershed stations (87.0 t/km^2/yr and 60.4 t/km^2/yr). Additionally, yields at the station farthest downstream (81.7 t/km^2/yr) were slightly larger than the yield calculated from the sum of both mid-watershed stations (74.6 t/km^2/yr), which together represented about 80% of the upstream drainage area.

Several additional patterns highlighting spatial heterogeneity of the system were observed. The ratio of sediment yields between the headwater stations increased steadily over time while the runoff ratio remained almost constant. Yields at one mid-watershed station were consistently higher than yields at the other mid-watershed station, despite similarity in runoff totals. Upstream watersheds show year-to-year variation in sediment yield. In contrast, yields at the farthest downstream station show minimal variation. This observation is consistent with the possibility that internal storage and remobilization tend to modulate downstream yields even with spatial and temporal variation in upstream sources. Observable inconsistencies in sediment yields between subwatersheds at monthly time scales suggest that there is a substantial degree of heterogeneity in terms of sediment response to large storm events. Despite significant internal variability, the overall range of sediment yield values at each site was consistent with values reported for multiple urban mid-Atlantic Piedmont watersheds. Comparison with global values indicates that sediment yields from Dead Run are in the same general range as the 25% quartile of urban sediment yields.

1. Introduction

Sediment transport dynamics within a watershed are complex interactions of various processes, which are strongly influenced by both sediment sources and sediment transport paths. Development of the urban landscape, and the consequent alteration of both the morphology and hydrology of the affected watershed, has a marked influence on streamflow response to rainfall events and on sediment sources and pathways (Wolman, 1967; Leopold, 1968; Hammer, 1972; Graf, 1975; Booth, 1990; Leopold et al., 2005; Taylor and Owens, 2009). Previous studies have documented increased sediment loads during periods of rapid urbanization (Guy and Ferguson, 1962; Wolman and Schick, 1967; Yorke and Herb, 1978). Nelson and Booth (2002) calculated a 50% increase in sediment yield due to anthropogenic perturbations in a moderately sized urban watershed in western Washington State. Overall, depending on the balance between sediment supply and transport capacity, urbanization-associated alterations can lead to

* Corresponding author.
E-mail address: john.kemper@colostate.edu (J.T. Kemper).

https://doi.org/10.1016/j.geomorph.2019.03.018
0169-555X/

aggradation and bar formation, rapid bank erosion, channel incision, and instability and degradation of habitat (Wolman, 1967; Walsh et al., 2005).

In order to investigate questions of sediment transport dynamics within a watershed, several studies have documented temporal patterns of sediment at annual (Asselman, 2000; Horowitz, 2006; Meade and Moody, 2010), seasonal (Duan et al., 2013), monthly (De Girolamo et al., 2015; Zeiger and Hubbart, 2016), and event scales (Walling and Webb, 1982; Goodwin et al., 2003; Lawler et al., 2006; Smith and Dragovich, 2009) but few of these are for urban systems. Spatial variability of sediment yield has been analyzed to assess downstream changes in the balance between export and storage. Allmendinger et al. (2007) found that although upland erosion and channel enlargement contributed significantly to the sediment budget, around 50% was stored on floodplains, rather than transported out of the watershed. Similar work by Hupp et al. (2013) observed that although the upstream reaches of a rapidly urbanizing, fifth-order watershed in Virginia displayed high net erosion rates, downstream reaches showed net deposition. A sediment budget compiled for the same watershed indicated that 52% of total suspended sediment load was stored via floodplain deposition (Gellis et al., 2017). Although the initial phase of development typically provides excess sediment to the channel, various authors have argued that a substantial portion of urban sediment loads are derived from streambank erosion (Hammer, 1972; Leopold, 1973; Trimble, 1997; Allmendinger et al., 2007; Fraley et al., 2009; Devereux et al., 2010; Hupp et al., 2013; Gellis et al., 2017; Cashman et al., 2018).

Differences in the dominant processes within a watershed can have a direct impact on sediment yields, i.e., if sediment storage is significant, then yields may decrease with increasing catchment area, whereas if channel erosion dominates, then yields may increase with increasing catchment area (Birkinshaw and Bathurst, 2006). Because urban sediment yields exhibit high variability, potentially as a direct result of watershed characteristics (Wolman, 1967; Fraley et al., 2009), a study design that includes high-frequency sediment data across multiple spatial scales can elucidate patterns of spatial and temporal variability that may be caused by differences among watersheds at the same scale or by variations in the balance between sediment storage and remobilization with increasing watershed scale. This is the approach we have taken here. The goal of this study is to use quantified urban sediment yields and loads from near-continuous in-stream monitoring data to investigate patterns of spatial and temporal heterogeneity across several watershed scales within a small urban watershed.

2. Study area

The Dead Run (DR) watershed (Fig. 1b) is located in the inner-ring western suburbs of Baltimore, in Baltimore County, Maryland, USA. The system is a tributary of the Gwynns Falls (Fig. 1a), which drains into Baltimore Harbor and ultimately into the Chesapeake Bay. The dominant land use within the 14.2 km^2 watershed is urban, as characterized by 47% impervious cover. The catchment also contains portions of two major interstate highways.

The study design spans three watershed scales ranging from 1–2 km^2 headwater catchments (DR5, DR2), nested within 5–6 km^2 intermediate-sized watersheds (DR3, DR4), which both drain to the 14.2 km^2 DR Franklintown (DRKR) station (Fig. 1b). The subwatersheds are all highly developed (45–55% impervious surface cover) but characterized by varying degrees of stormwater management (SWM), ranging from 3 to 55% of catchment area treated. A substantial portion of the natural headwaters of the drainage network has been buried in storm drains. Despite this, modified floodplains occur in several areas of the catchment. Evidence of sediment deposition is apparent in a number of locations, particularly upstream and downstream of culverts and road embankments (Fig. 2a). Quasi-natural floodplains are only observed in the lower portion of the watershed, downstream of the confluence of DR3 and DR4. There is noticeable bank erosion, particularly within the older-developed DR5 subwatershed (Fig. 2b). There is

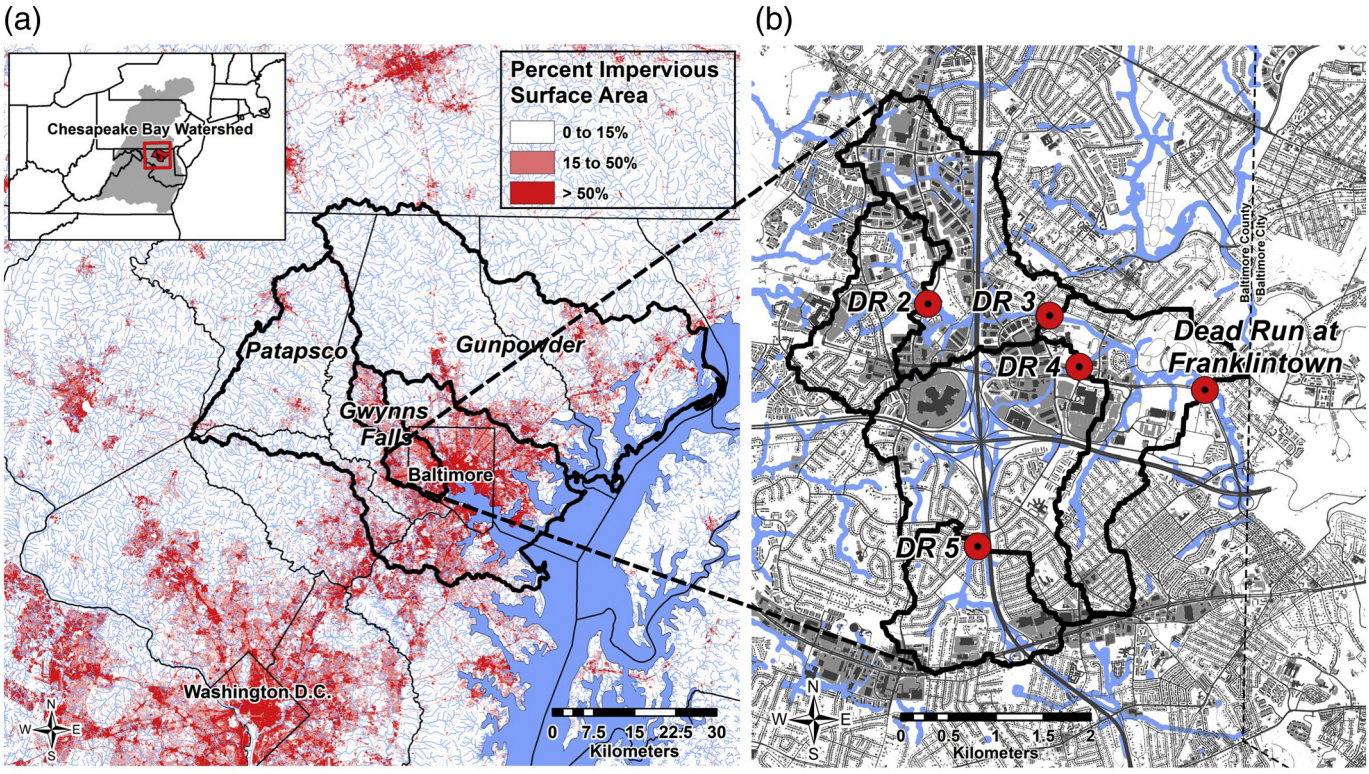

Fig. 1. (a) Regional location of study area in the Chesapeake Bay watershed, where red shading indicates percent impervious surface area; (b) Dead Run watershed (14.2 km^2 area) in suburban Baltimore, MD. Red dots indicate USGS gaging stations where turbidity and discharge were recorded. DR2 drains to DR3; DR5 drains to DR4; DR3 and DR4 drain to Dead Run Franklintown (DRKR). Map credit: John J. Lagrosa IV, Center for Urban Environmental Research and Education, University of Maryland, Baltimore County.

Fig. 2. (a) Gravel bars downstream of a culvert (photograph by C. Welty). Two of the three culvert "barrels" are filled with sediment. (b) Gully in the DR5 subwatershed (photograph by A.J. Miller).

observable spatial heterogeneity within the system, highlighted by several key watershed characteristics, as summarized in Table 1.

The typical hydrologic response of the Dead Run subwatersheds to a rainfall pulse is depicted in Fig. 3, which shows hydrographs associated with a high-intensity short-duration summer thunderstorm occurring on 23 June 2015. Response times from peak rainfall intensity to peak discharge ranged between 15 and 20 min for 1–2 km^2 watersheds to ~1 h at 14 km^2. Despite significant differences in stormwater management across the subbasins, all subwatersheds display a flashy hydrologic response.

Because the subwatersheds in this study exhibit different development patterns and extent of stormwater management practices, comparison and evaluation of suspended sediment loads across equivalent

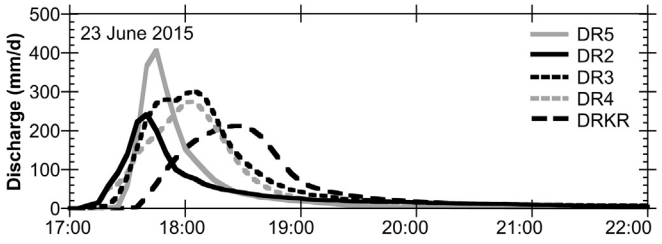

Fig. 3. Hydrographs depicting the typical responses to a precipitation event (23 June 2015) for the Dead Run subwatersheds. Precipitation began at 17:15 on 23 June 2015.

subwatershed scales (DR2-DR5, DR3-DR4), as well as in the downstream direction (DR5-DR4-DRKR; DR2-DR3-DRKR), can provide insight into sediment transport dynamics in characteristically heterogeneous urban watersheds.

3. Methods

In-stream turbidity sensors, streamflow data, and suspended sediment samples are commonly used to construct time-series of suspended sediment concentrations (Langlois et al., 2005; Lawler et al., 2006; Horowitz, 2008, 2009; Mather and Johnson, 2014; Yeshaneh et al., 2014). Once constructed, suspended sediment time series can be combined with measured discharge time series to calculate sediment loads and yields and to examine and evaluate patterns of sediment delivery.

3.1. Data collection

Stream stage was recorded at four U.S. Geological Survey (USGS) gaging stations (DR2-DR5) using Accububble pressure devices and at DRKR using a radar device. Gaging station characteristics are summarized in Table 2. Stage-discharge relations were developed by USGS following published methods (Rantz et al., 1982a, 1982b). Stage data were collected at five-min intervals to capture the flashy nature of the urban Dead Run streams.

Water quality data were collected by YSI EXO2 sondes co-located with the USGS stream gaging stations. The sondes were equipped with nephelometric near-IR turbidimeter sensors, having a detection range of 0 to 4000 FNU (formazin nephelometric units) with a precision of 0.01 FNU and accuracy of 0.3 FNU or ± 2% of reading. The sensors were calibrated regularly using a 2-point calibration with distilled water and YSI turbidity calibration solution (item 607300 (124 FNU)). Turbidity data were collected at 30-min intervals from December 2012 through November 2014 at DR5, through December 2014 at DR2, through February 2015 at DR3, through March 2015 at DR4, and through May 2015 at DRKR. Data were collected at five-minute intervals subsequent to those dates at each monitoring station.

The USGS has developed methods for the collection of fluvial sediment data (Guy, 1969; Porterfield, 1972; Edwards and Glysson, 1999; Nolan et al., 2005; Diplas et al., 2008; Rasmussen et al., 2011), which were followed in this study. Sediment samples were gathered at all five USGS stream gaging stations (Table 2). At least seven point samples per year were collected at each station over a range of storm magnitudes. Point samples were gathered using an ISCO 6712 automated

Table 1
Dead Run subwatershed characteristics.

Subwatershed	Area (km^2)	Mean basin slope	Nested within	% Impervious Surface Cover	% Tree canopy	% Herbaceous cover	% Stormwater management
DR5	1.63	0.0390	DR4	45.0	31.9	24.7	2.70
DR2	1.92	0.0469	DR3	49.0	24.6	27.7	33.0
DR3	5.09	0.0492	DRKR	55.1	23.4	23.1	55.4
DR4	5.84	0.0435	DRKR	47.1	27.7	26.4	9.30
DRKR	14.2	0.0467		47.1	28.1	26.1	36.2

Table 2
Dead Run stream gage locations and summary of hydrologic characteristics.

Station	Year Established	USGS Station	Average annual flow (m^3/s)	Peak flow (m^3/s)	Date of peak flow	Peak turbidity (FNU)	Peak sample concentration (mg/L)
DR5	2007	1589312	0.0300	34.6	7/30/2016	1060	1650
DR2	2008	1589316	0.0340	29.2	7/30/2016	865	650
DR3	2008	1589320	0.109	82.5	7/30/2016	703	540
DR4	2007	1589315	0.118	105	7/30/2016	1080	1230
DRKR	1959	1589330	0.246	210.	6/22/1972	857	1590

sampler. Four seasonal baseflow samples were collected using the same method.

Equal-Weight Increment (EWI) samples were collected at each gaging station for two medium- to high-flow events during the first two years of the study by lowering a DH-81 sampler at multiple verticals across the channel at the nearest possible location to the gaging station (Edwards and Glysson, 1999; Nolan et al., 2005; Gray and Simões, 2008). Between 10 and 20 verticals were designated for each location, as recommended by USGS sampling guidelines. These EWI samples were compared to the ISCO samples in order to determine the efficiency of point sampling and to relate sediment concentrations from the ISCO to those from EWI sampling. EWI sample concentrations were within 5% of ISCO point sample concentrations for the same storm event at all stations except for DR4, where they were within 15%. This indicates that sediment concentrations were well mixed across the channel. Samples were shipped to the USGS Kentucky Water Science Center Sediment Laboratory for analysis of suspended sediment concentration following standard USGS methods (Guy, 1969; Knott et al., 1992; Shreve and Downs, 2005).

3.2. Data analysis

Suspended sediment concentration-turbidity relations were developed for each station, based on sediment concentration data from the samples analyzed by the USGS laboratory and the time-associated, in-stream measured turbidity (Fig. 4). Turbidity-concentration relations were then used in conjunction with turbidity time series data from the in-stream sensors to construct time series of suspended sediment concentration following the published USGS method (Rasmussen et al., 2011) (Fig. 5).

Suspended sediment concentration and stream discharge data were combined to calculate suspended sediment loads for 2013–2016. Daily, monthly, and annual suspended sediment loads (SSL) were calculated by the integration of loads over each measured time interval. Suspended sediment yields (SSY) were calculated by the division of suspended sediment loads by drainage area.

Days with missing or erroneous values (e.g., from probe burial during storm events) were removed from the record and filled in as follows. Daily suspended sediment yield was plotted as a function of mean daily discharge (Fig. 6) and peak daily discharge to examine any differences in the predictive power of these relations. A simple power function was fitted to each data set, and each displayed similar R^2 values, suggesting that mean daily discharge is equally as good a predictor of daily suspended sediment yield as peak daily discharge. An empirical model for each station was then developed using a power law regression of mean daily discharge vs daily suspended sediment load for the 100 largest storms of the monitoring period (Fig. 7). This was done in order to fill gaps in the data so as to calculate annual loads. The 100 largest storms were chosen in order to avoid disproportionate influence of baseflow days on the load-discharge relationship; good fits for large events were chosen at the expense of poorer baseflow fits. Mean daily discharge was chosen because USGS provides estimates of mean daily discharge for days with missing data following well-established methods (Sauer, 2002). Model error is summarized in Table 3. Error

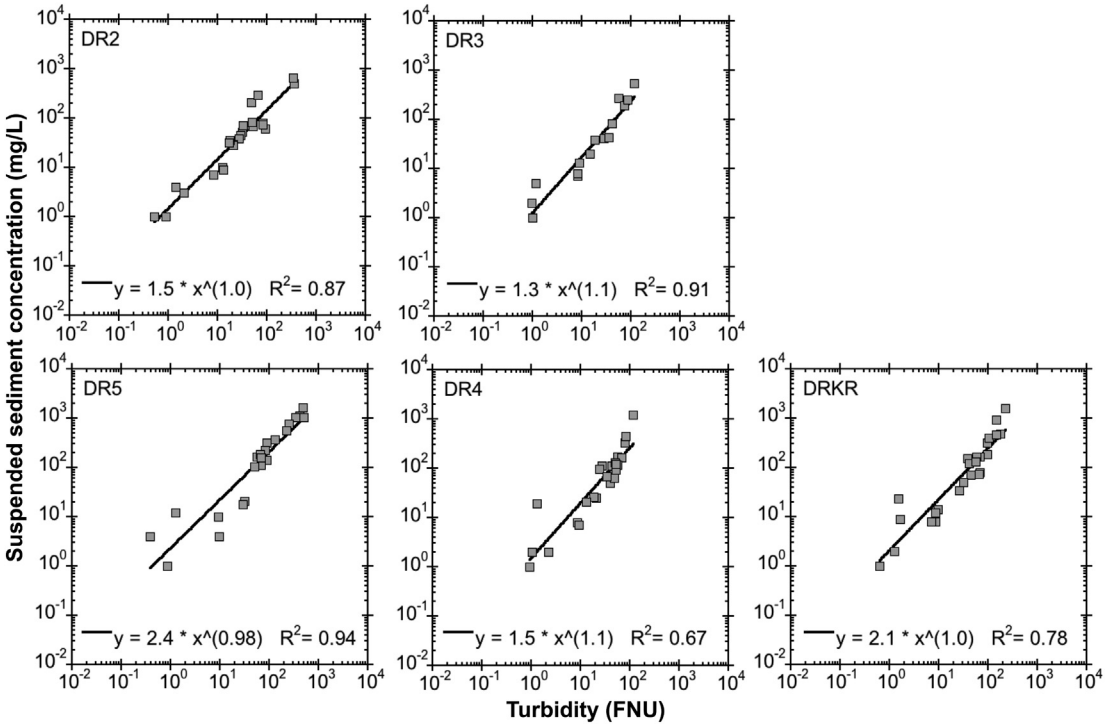

Fig. 4. Suspended sediment concentration-turbidity relations for the five Dead Run subwatersheds.

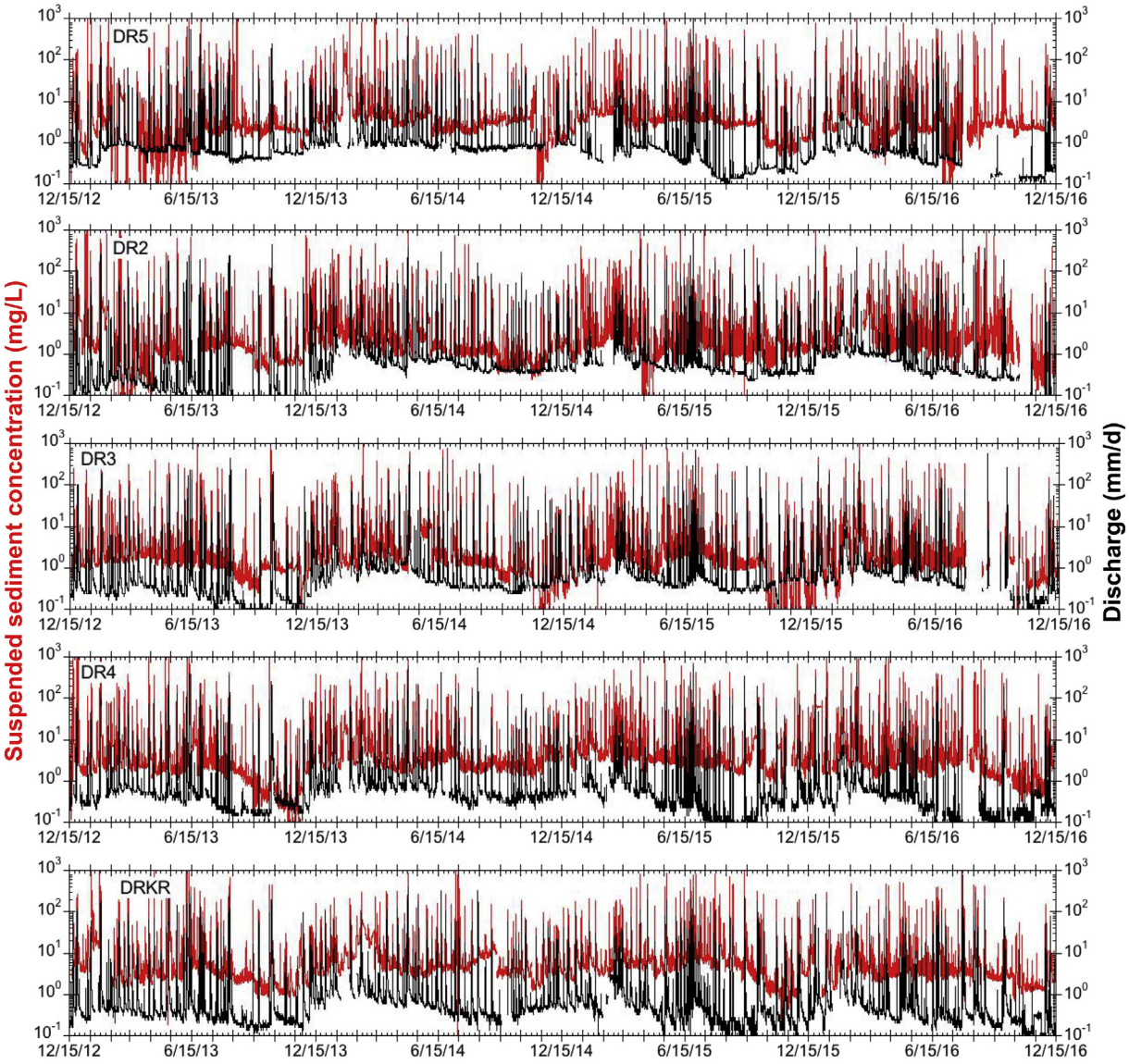

Fig. 5. Suspended sediment concentration time series for the five Dead Run subwatersheds.

for events that fall outside the range of our model, i.e., the largest storm events missed due to extreme floods that resulted in power loss to the equipment, cannot be estimated. The statistical significance of spatial and temporal differences in loads and yields was investigated at the annual scale by fitting a two-way linear model to the annual data and calculating unadjusted *p*-values for pairwise comparisons. At the monthly scale, unadjusted p-values for pairwise comparisons were calculated using a randomized block design.

4. Results

Sediment yields for each subwatershed at monthly and annual timescales are provided below. Here, we present simple "base" results; discussion of the differences highlighted by these simple results and the more derivative metrics used to investigate these differences are addressed in subsequent sections.

4.1. Annual yields

Annual suspended sediment yields were calculated for each station (Fig. 8, Table 4). The four tributary stations displayed substantial variation in yield from year to year. For the DR5 and DR3 stations, 2013 had the lowest sediment yield out of the four years, whereas for the DR2 and DR4 stations, 2015 had the lowest sediment yield (Table 4). Relative magnitudes of sediment yield between paired watersheds of similar size (e.g., DR5 vs DR2 and DR3 vs DR4) follow a consistent trend from year to year. Annual yields at DR5 and DR4 are higher than at DR2 and DR3, respectively, for all four years of record. Average annual yield (Table 4) was higher at DR5 than at DR2, and higher at DR4 than DR3, to statistically significant levels (p-values <0.05). Comparing yields across watershed scales, yields were higher at DR3 than at its tributary (DR2) in all years, while yields at DR4 were higher than at its tributary (DR5) for all years except 2016. Although patterns in annual yield between upstream and downstream stations are of interest, average annual yields are not different to statistically significant levels (p-values >0.05). The DRKR gage had a lower annual sediment yield than DR4 in three of the four years (with the exception of 2015) and was larger than DR3 in all four years. Annual yields are more similar between DR4 and DRKR than between DR3 and DRKR. The differences in average annual yield between DR3 and DRKR and between DR4 and DRKR are not statistically significant (p-values >0.05).

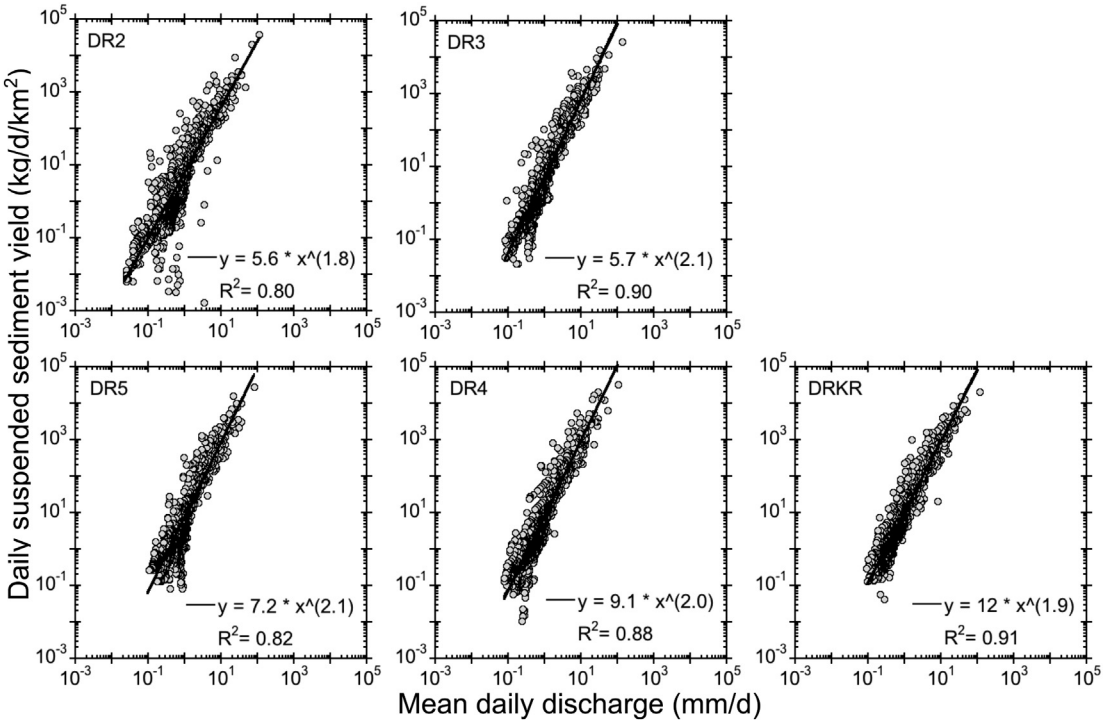

Fig. 6. Correlation between mean daily discharge and daily suspended sediment yield for the five study watersheds.

4.2. Monthly yields

Monthly suspended sediment yields were calculated across the four-year sampling period of 2013–2016 in order to examine the temporal organization of suspended sediment transport within the catchment (Fig. 9). Monthly yields varied by over two orders of magnitude across all stations and show little evidence of any interannual patterns. The data display a seasonal pattern: months between November and March had lower sediment yields than months between April and October for the four tributary gage sites, with only a few exceptions across the four years of record. The largest monthly sediment yields are less extreme with increasing watershed scale.

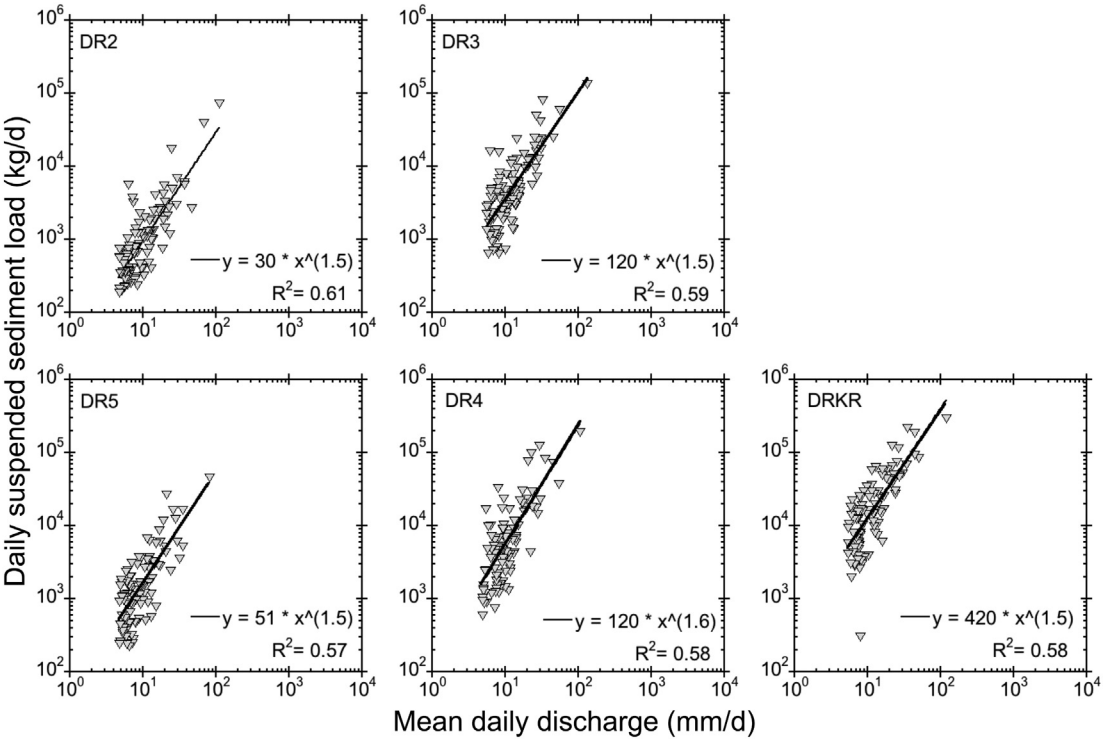

Fig. 7. Daily suspended sediment load as a function of mean daily discharge for the 100 largest storms at each of the five Dead Run monitoring stations.

Table 3
Coefficients of determination and empirical error estimates based on residuals from regression models of daily suspended sediment load as a function of mean daily discharge for the 100 largest storms at each station.

Subwatershed	Mean average error (tons)	Root mean square error (tons)	R^2
DR5	0.16	0.86	0.57
DR2	0.13	1.3	0.61
DR3	0.44	2.6	0.59
DR4	0.73	5.3	0.58
DRKR	1.4	8.7	0.58

For the four upstream stations, several months stand out as having the highest yields and are associated with major floods recorded during the study period: the storm of 30 April 2014 is associated with a month that has among the highest yields in the record at four of the five gage sites. The flood of 30 July 2016 stands out at DR5, DR2, and DRKR (to a lesser extent). As this was the largest flood for the monitoring period at all five stations, it is notable that this storm produced the largest yield at only one station (DR5). Because the gaging equipment was inundated by this event at DR3, DR4, and DR5, sediment loads for this event were estimated using the method discussed above in Section 3.2. The flood event of 10 Oct 2013 stands out at DR3 and DR4 but not at the headwater tributary sites. The flood of 30 Jan 2013 stands out at DR4 and to a lesser extent at DR3, and the 23–24 Feb 2016 event stands out at DR5, DR4, and DR3. The 27 June 2016 event is notable at all stations except DR2.

For the two headwater stations, the overall monthly maximum for the entire monitoring period occurred in different years (July 2016 for DR5 vs April 2014 for DR2). Annual monthly maxima also appear to represent a larger fraction of total annual load at DR2 than at DR5, accounting for between 21 and 63% of the annual suspended sediment load versus 15 and 25%, respectively. The mid-watershed DR3 and DR4 gages are located only about 500 m apart, yet only three of the top five monthly suspended yields at each station were also among the top five at the other station. Annual monthly maxima at DRKR have less variability than at DR3 and DR4, and the overall second highest monthly load at the mid-watershed stations (Feb 2016) was only the fifth highest at DRKR.

5. Discussion

The annual sediment yield results and the comparison of monthly sediment yields among stations indicate a substantial degree of heterogeneity within a highly impervious watershed of such small cumulative drainage area. In order to better understand possible drivers of the observed patterns we present several different comparative analyses of our sediment yield data sets.

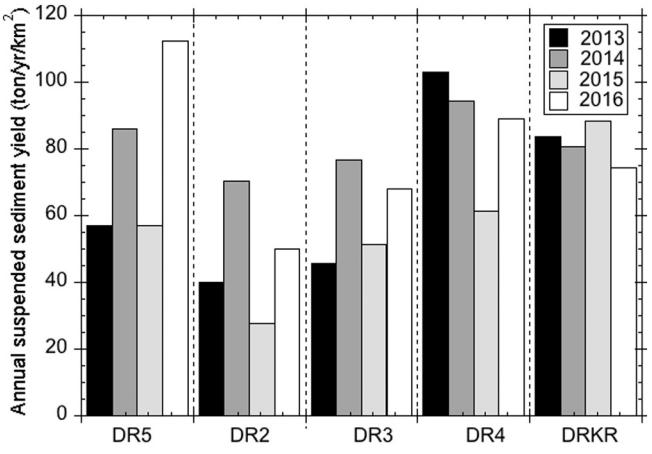

Fig. 8. Annual suspended sediment yields, 2013–2016, at the five Dead Run stations.

Table 4
Annual suspended sediment yields and runoff at the five Dead Run stations.

	Annual suspended sediment yields ($t/km^2/yr$)					
Station	2013	2014	2015	2016	Mean	Standard deviation
DR5	57.0	86.1	57.1	112	78.2	23.1
DR2	40.0	70.3	27.5	50.2	47.0	15.7
DR3	45.6	76.7	51.3	68.0	60.4	12.5
DR4	102	94.4	61.5	89.0	87.0	15.6
DRKR	83.7	80.7	88.2	74.3	81.7	5.06
	Annual Runoff (mm)					
DR5	624	837	486	653	649	144
DR2	567	805	559	591	630.	116
DR3	585	822	657	686	688	99.4
DR4	641	797	618	572	657	97.9
DRKR	667	842	612	628	678	106

5.1. Frequency analysis and the role of large storms

In order to assess the relative importance of transport by large storms as a fraction of cumulative sediment yield across our study watersheds, we developed empirical frequency distributions for suspended sediment data sets at each gage site. The daily sediment yield values were sorted from largest to smallest and a cumulative sum was calculated for each value in order to plot a cumulative frequency distribution for sediment yield. Fig. 10 illustrates this frequency distribution for all five of the gage sites. Curves that are farther to the right require more time to move an equivalent fraction of total sediment as compared with curves that are farther to the left. Table 5 includes a summary of the number of days per year required to transport 50%, 75% and 90% of the total sediment yield. The time required to transport 50% of the sediment ranged between two and five days per year; for 75% of cumulative transport the values ranged from 11 to 14 d/yr; and for 90% of cumulative transport a total of 25 to 31 d/yr were required. The downstream Franklintown site (DRKR) required the largest number of days per year to move 50% of its annual load. The fraction of total sediment yield moved in 1% of the time was largest at DR2 and DR4 and smallest at DRKR. The pattern illustrated in Fig. 10 shows that the total annual sediment load was concentrated over a smaller number of days per year for DR2 by comparison with DR5, DR4 and DR3, and was generally spread over a larger number of days at DRKR. DR2 rarely moves significant amounts of sediment and likely has less sediment available to be mobilized than the other stations.

These temporal differences may be related to the relative availability of sediment to be transported; sediment sources upstream may be more infrequently accessed compared to DRKR, where sediment sources may be more readily accessible, perhaps from in-channel deposits as we suggest in section 5.3 below. The available data suggest that sediment transport at DRKR is less dependent on large storms than may be the case at some of the upstream stations

5.2. Hydrology as a driver of spatial heterogeneity

It is clear from the analysis presented in Section 5.1 that large storms are responsible for a substantial fraction of the cumulative sediment transport in most of our study watersheds, although their relative importance may vary between stations and across watershed scales. Given the small size of the watershed even at the Franklintown gage, it would appear reasonable to assume that the hydrologic events driving patterns of sediment yield should have relatively uniform impacts across all the stations, from Franklintown upstream to the headwater gages. However, there are inconsistencies in the pattern of comparative sediment yield values observed among stations. For this reason we have

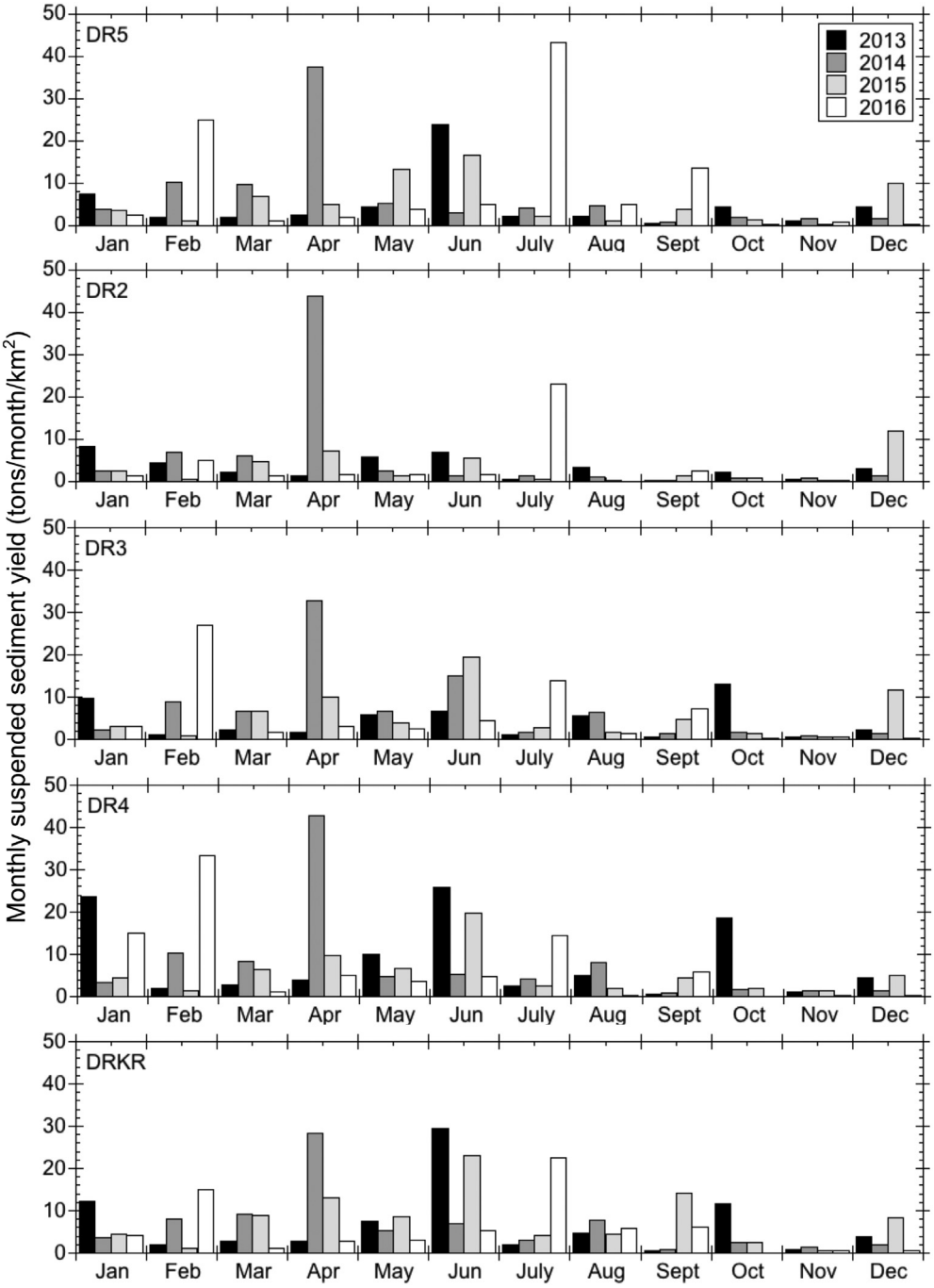

Fig. 9. Monthly suspended sediment yields at the five Dead Run stations.

evaluated the spatial and temporal distribution of runoff and relations between runoff and watershed area. The ratio of upstream runoff to downstream runoff is roughly proportional to the ratio of watershed area (Table 6), which suggests that each subwatershed contributes a proportionally consistent amount of runoff on an annual basis. Annual average runoff was higher for DR3 than for DR4, but higher for DR5 than for DR2, although neither difference is statistically significant (p-value >0.05). While the discrepancy in runoff totals between DR5 and DR2 may account for some of the variability in sediment yields between the two headwater stations, the magnitude of the difference in average annual runoff (~3%) is likely not sufficient to explain the statistically significant difference in sediment yield (~40%). These differences in yield between the two headwater stations may be a function of development age and relative extent of stormwater management; older development and less extensive stormwater management within the DR5 subwatershed may result in greater degradation of the channel (Fig. 2) than in the DR2 subwatershed, which would in turn lead to a more substantial source of sediment in the form of bank erosion in DR5 than in DR2.

Average annual suspended sediment yield is significantly higher (p-value <0.05) at DR4 than at DR3 despite no statistically significant difference in runoff. Overall, spatial and temporal disparities in suspended sediment load do not appear to track with patterns of hydrologic response. This suggests that there is some additional complexity governing sediment yields, perhaps in the form of sediment storage and remobilization, discussed further in Section 5.3.

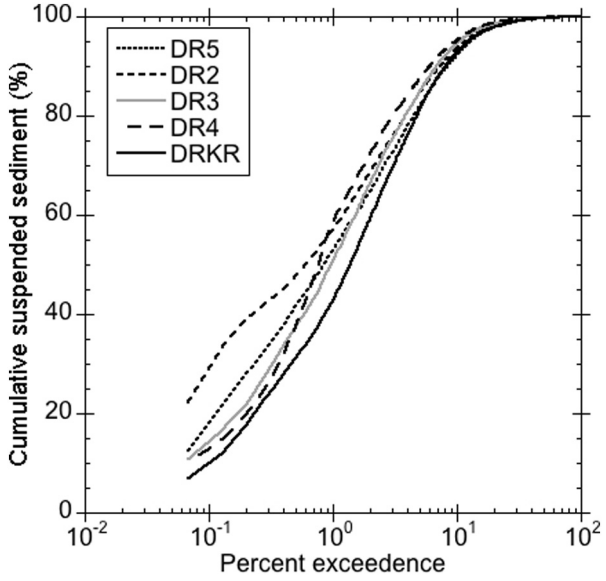

Fig. 10. Percent exceedance of cumulative suspended sediment at the five Dead Run stations, 2013–2016.

5.3. Paired watershed and upstream-downstream sediment relationships

As stated in the preceding discussion, the spatial variability of sediment yields is likely minimally driven by a heterogeneous hydrological response. In order to more fully investigate additional influencing factors, several comparisons of sediment yield were made, both at equivalent watershed scales and in the downstream direction. Ratios of suspended sediment yield for each year are summarized in Table 7. The DR5/DR2 SSY ratio increased over time, a trend that is not reflected by annual runoff totals. On the other hand, for the downstream mid-sized watershed pairing of DR4/DR3, the SSY ratio increased substantially from 2013 to 2014 but has remained roughly stationary since. We developed double mass curves of cumulative yield for each watershed pair to more fully investigate these dynamics (Fig. 11a). For the DR5/DR2 pairing, a clear departure from the 1:1 line occurs in June 2013, at which point yields at DR5 are consistently higher than at DR2. An additional break in trend occurs in April 2014. Subsequent yields at DR5 are increasingly higher than DR2, a trend that is not reflected in runoff totals for the same time period (Fig. 11b). For the DR3/DR4 pairing, yields are substantially higher at DR4 than DR3 until April–June 2014, where yields are roughly equivalent at both stations. Post-June 2014 the DR4/DR3 cumulative yield ratio remains approximately consistent. From these trends, it is evident that sediment mobilization is episodic and that the two watershed pairings are not responding exactly in tandem. Noticeable differences in the timing and occurrence of large monthly suspended sediment yields further support this conjecture (Fig. 9). As discussed previously, these discrepancies in sediment yield across equivalent watershed scales may be the result of a difference in sediment availability in each subwatershed.

Table 7
Sediment yield ratios and runoff ratios across Dead Run subwatersheds.

Watershed pair	2013	2014	2015	2016	Annual average
Suspended sediment yield					
DR5/DR2	1.43	1.23	2.07	2.24	1.66
DR4/DR3	2.26	1.23	1.20	1.31	1.44
Runoff					
DR5/DR2	1.11	1.04	0.868	1.11	1.03
DR4/DR3	1.10	0.970	0.940	0.833	0.960

Loads were examined to investigate the relative impact of each upstream station on the station immediately downstream (Table 6). Annual average load ratios are essentially equivalent for the DR5/DR4 nested pair and for the DR2/DR3 nested pair. Thus a nearly equivalent proportion of the downstream suspended sediment load was derived from the two upstream headwater stations, and may indicate that DR5 does not have a larger impact on loads at DR4 than DR2 does on loads at DR3. The load ratio for DR4/DRKR is noticeably higher than DR3/DRKR.

Sediment yields at DRKR are noticeably less variable over the four years of record than annual runoff, and less variable than the yield from DR3 and DR4 combined. We note in particular that between 2014, a very wet year, and 2015, a drier year, every station other than DRKR experienced a significant decrease in sediment yield whereas DRKR shows a slight increase. We constructed a double-mass curve where cumulative monthly suspended sediment load at DRKR is plotted against the combined cumulative monthly suspended sediment loads at DR3 and DR4 (Fig. 12a). The regression line represents the average trend but individual points are not randomly distributed around that trend; rather there are series of points that lie above or below the line. The trend line represents the predicted value of cumulative sediment load at DRKR based on the sum of loads at DR3 + DR4. We subtracted the predicted values from the actual DRKR values to derive cumulative departures from the average relationship between suspended sediment load at DRKR and the sum of suspended loads at DR3 + DR4 (Fig. 12b). The figure suggests that there is a cyclical pattern of sediment storage upstream of DRKR (i.e., DRKR sediment load is less than predicted by the sum of DR3 + DR4) followed by remobilization of sediment from storage (i.e., DRKR sediment load is more than predicted by the sum of DR3 + DR4). The time scale of these fluctuations indicates that the sediment is in temporary rather than long-term storage, which would most likely be in the channel where it is relatively accessible to future erosion.

Table 5
Number of days required to move 50%, 75%, and 90% of the total annual sediment load in Dead Run subwatersheds.

	Days to move		
Subwatershed	50% total SSL (d/yr)	75% total SSL (d/yr)	90% total SSL (d/yr)
DR5	3	13	31
DR2	2	11	27
DR3	4	11	25
DR4	3	11	27
DRKR	5	14	30

Table 6
Ratios of average annual runoff, average annual suspended sediment load, and watershed area for the five Dead Run subwatersheds.

Upstream/downstream	Annual $runoff_{upstream}$/Annual $runoff_{downstream}$	Annual $SSL_{upstream}$/Annual $SSL_{downstream}$	Watershed $area_{upstream}$/Watershed $area_{downstream}$
DR5/DR4	0.28	0.25	0.28
DR2/DR3	0.35	0.29	0.38
DR3/DRKR	0.36	0.27	0.36
DR4/DRKR	0.40	0.44	0.41
(DR3 + DR4)/DRKR	0.76	0.70	0.77

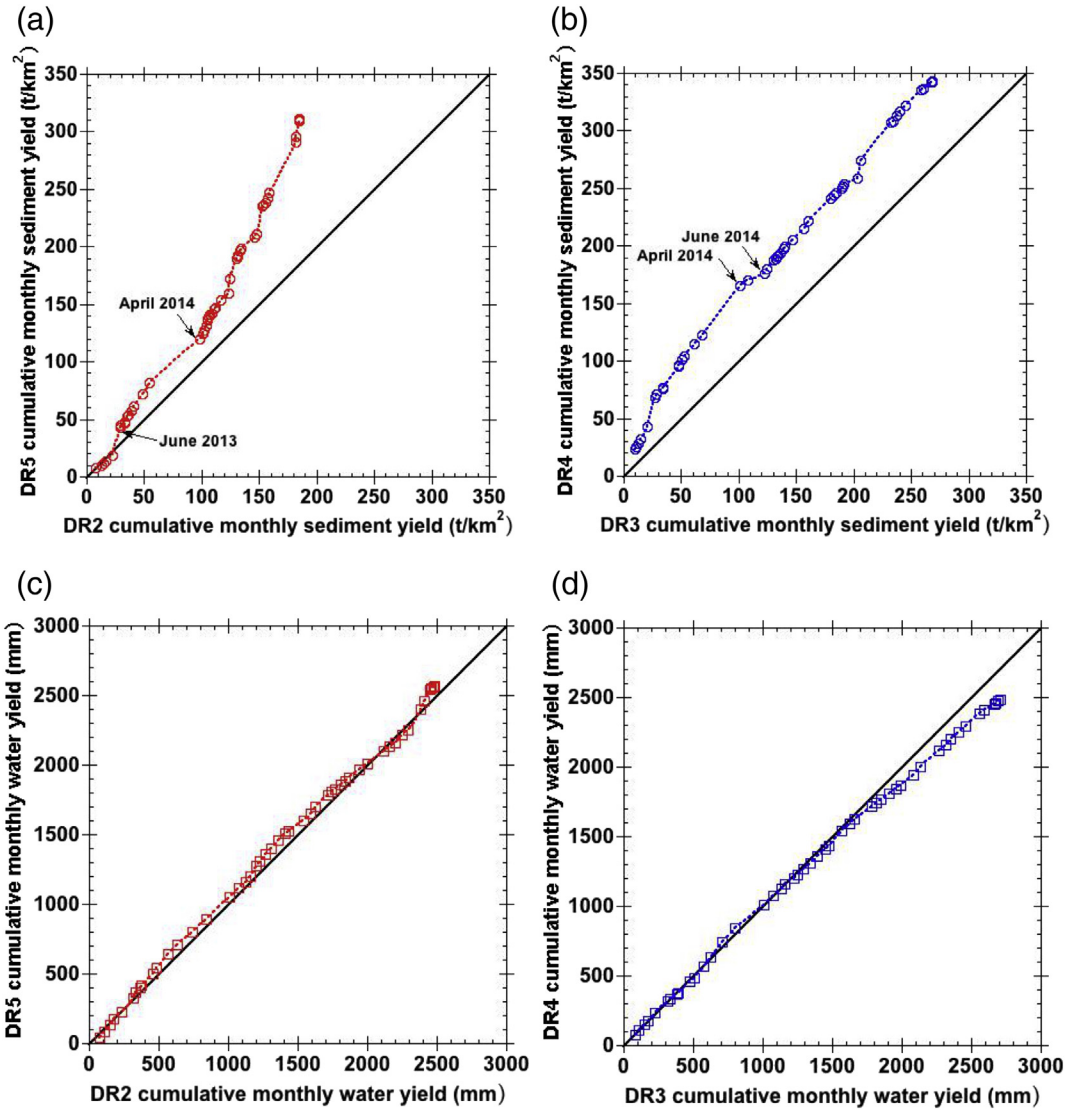

Fig. 11. Cumulative monthly sediment yield for paired watershed sites for (a) DR5 and DR2 (headwatersheds) and (b) DR4 and DR3 (mid-watersheds); cumulative monthly water yield for paired watershed sites for (c) DR5 and DR2 and (d) DR4 and DR3. 1:1 ratio indicated by black line.

Overall, this trend suggests that there is some modulation of loads at DRKR relative to its tributaries and alternating storage and remobilization appears to be the most likely explanation. Several sites of potential in-channel storage exist; there are a number of in-channel bars upstream of culverts and even on top of concrete slabs (Fig. 13).

5.4. Comparison to other sites

Despite the internal variability of our annual sediment yield values, the overall range of sediment yield values at the Dead Run gage sites is consistent with values tabulated by Fraley et al. (2009, Table 5) for other mid-Atlantic Piedmont sites, including multiple urban watersheds, with the exception of a few higher outliers representing the early construction phase of elevated sediment yield. Our results are lower by about a factor of five compared with the highest urban values reported by Gellis et al. (2005) for the Chesapeake Bay watershed and Gellis et al. (2017) for the suburban Difficult Run watershed in northern Virginia. Comparison with values tabulated by Russell et al. (2017, Table 2) indicates that sediment yields from Dead Run are in the same general range as the 25% quartile of a global set of urban sediment yields representing 13 studies and 22 data points.

6. Conclusions

Continuous monitoring of suspended sediment concentrations and discharge in the Dead Run watershed allowed patterns of sediment transport dynamics to be investigated across a variety of spatial and temporal scales in an urban environment. Although several studies exist that document the impacts of urbanization on sediment yields (Guy and Ferguson, 1962; Wolman and Schick, 1967; Yorke and Herb, 1978; Nelson and Booth, 2002) and attempt to identify sources of sediment within urban environments (Trimble, 1997; Pizzuto et al., 2000; Allmendinger et al., 2007), few studies have used continuous monitoring to quantify urban sediment yields (Lawler et al., 2006; Horowitz, 2008).

The watershed displayed suspended sediment characteristics common to most watersheds, as it was highly influenced by relatively infrequent large storm events. Interestingly, the effect of large storms does not appear to be consistent across subwatersheds. Large suspended sediment yields in one subwatershed were not necessarily observed across all other subwatersheds during the same storm event, i.e., there is a heterogeneous response in terms of subwatershed sediment yield despite similar hydrologic response. Yield ratios for the headwater stations (DR5 and DR2) were increasingly disparate with time, while yield ratios

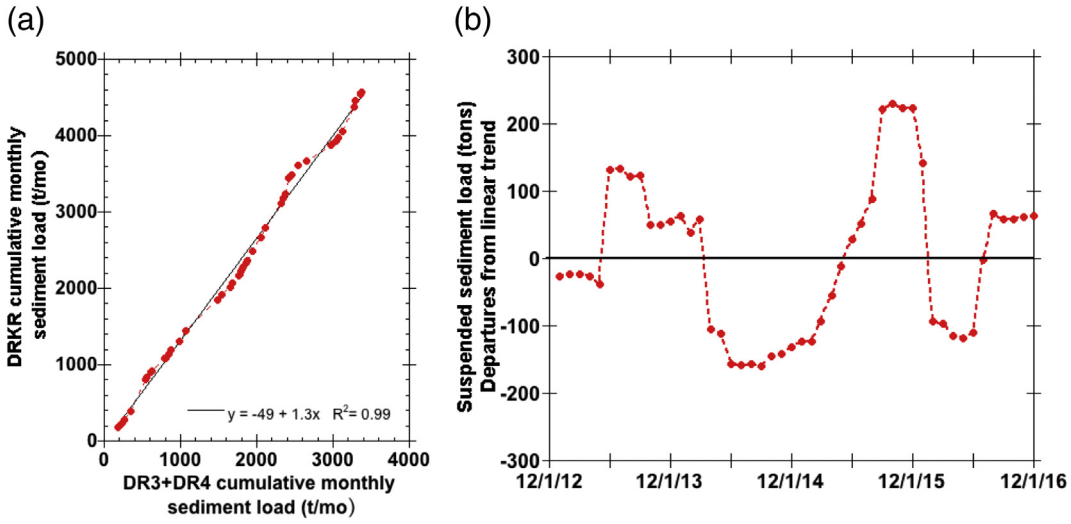

Fig. 12. (a) Cumulative monthly sediment load for DR3 + DR4 vs DRKR fitted with a linear trend; (b) residuals from (a) as a function of time.

for the mid-watershed stations (DR3 and DR4) were more consistent. Yields for the farthest downstream station (DRKR) displayed much less interannual variability than the upstream tributary stations. Our analysis suggests that dynamic storage and remobilization of sediment between sites modulates the downstream delivery of sediment.

Fig. 13. (a) An in-channel bar upstream of a culvert and (b) vegetated in-channel bars on top of a fully concrete channel. (Photos by A.J. Miller).

Departures from the average relationship between sediment loads at DR3 + DR4 and DRKR are cyclical in nature and further support this idea.

In terms of the insights that can be gleaned from these observations, the inconsistent influence of large storm events across subwatersheds suggests that the dominant sources of sediment could be more frequently accessible in some subwatersheds than others, e.g., in-channel deposits or bank sediment versus other sources. The evident role of sediment storage suggests that measurable changes in upstream tributary behavior may not be detected at the watershed mouth for several years. Further investigation is needed in order to determine the drivers of suspended sediment yield within each subwatershed.

The fine-scale design of this study represents a unique opportunity to compare and contrast sediment yields across a variety of spatial and temporal scales, and provides insight into sediment transport dynamics within an urbanized watershed. The patterns observed here, and subsequent conclusions drawn, should advance the understanding of the fate and transport of sediment in urban landscapes, and support the idea that sediment storage plays a significant role within urban systems. Finally, this study emphasizes the value of continuous monitoring at multiple sites in order to fully quantify catchment-scale sediment dynamics.

Acknowledgements

This work was supported by the Chesapeake Bay Trust [grant # 12507]. C. Welty's time was also supported in part by NSF cooperative agreements CBET 1444758 and BCS 1444755. The authors are grateful to Erin Stapleton, Matthew Schley, Maurice Brown, and Nicholas Rynes for assistance with field work, as well as reviewers Kathryn Russell and Avijit Gupta for their constructive comments. Field data are available at https://doi.org/10.4211/his-5653.

References

Allmendinger, N.E., Pizzuto, J.E., Moglen, G.E., Lewicki, M., 2007. A sediment budget for an urbanizing watershed, 1951-1996, Montgomery County, Maryland, U.S.A. J. Am. Water Resour. Assoc. 43, 1483–1498. https://doi.org/10.1111/j.1752-1688.2007.00122.x.

Asselman, N.E.M., 2000. Fitting and interpretation of sediment rating curves. J. Hydrol. 234, 228–248. https://doi.org/10.1016/S0022-1694(00)00253-5.

Birkinshaw, S.J., Bathurst, J.C., 2006. Model study of the relationship between sediment yield and river basin area. Earth Surf. Process. Landf. 31, 750–761. https://doi.org/10.1002/esp.1291.

Booth, D.B., 1990. Stream-channel incision following drainage-basin urbanization. J. Am. Water Resour. Assoc. 26, 407–417. https://doi.org/10.1111/j.1752-1688.1990.tb01380.x.

Cashman, M.J., Gellis, A., Gorman- Sanisaca, L., Noe, G.B., Cogliandro, V., Baker, A., 2018. Bank-derived material dominates fluvial sediment in a suburban Chesapeake Bay watershed. River Res. Appl. 34, 1032–1044. https://doi.org/10.1002/rra.3325.

De Girolamo, A.M., Pappagallo, G., Lo Porto, A., 2015. Temporal variability of suspended sediment transport and rating curves in a Mediterranean river basin: the Celone (SE Italy). CATENA 128, 135–143. https://doi.org/10.1016/j.catena.2014.09.020.

Devereux, O.H., Prestegaard, K.L., Needelman, B.A., Gellis, A.C., 2010. Suspended-sediment sources in an urban watershed, Northeast Branch Anacostia River, Maryland. Hydrol. Process. 24, 1391–1403. https://doi.org/10.1002/hyp.7604.

Diplas, P., Kuhnle, R., Gray, J.R., Glysson, G.D., Edwards, T.K., 2008. Sediment transport measurements. In: Garcia, M.H. (Ed.), Sedimentation Engineering: Processes, Measurements, Modeling and Practice. American Society of Civil Engineers, Manuals and reports on engineering practice no. 110, Reston, VA, 307–353.

Duan, W., Takara, K., He, B., Luo, P., Nover, D., Yamashiki, Y., 2013. Spatial and temporal trends in estimates of nutrient and suspended sediment loads in the Ishikari River, Japan, 1985 to 2010. Sci. Total Environ. 461–462, 499–508. https://doi.org/10.1016/j.scitotenv.2013.05.022.

Edwards, T.K., Glysson, G.D., 1999. Field methods for measurement of fluvial sediment U.S Geological Survey Techniques of Water-Resources Investigations, Book 3. Chapter C2, 97.

Fraley, L.M., Miller, A.J., Welty, C., 2009. Contribution of in-channel processes to sediment yield of an urbanizing watershed. J. Am. Water Resour. Assoc. 45, 748–766.

Gellis, A.C., Banks, W.S.L., Langland, M.J., Martucci, S.K., 2005. Summary of suspended sediment data for streams draining the Chesapeake Bay watershed, Water Years 1952–2002. U.S. US Geol. Surv. Sci. Investig. Rep. 2004-5056, 59.

Gellis, A.C., Myers, M.K., Noe, G.B., Hupp, C.R., Schenk, E.R., Myers, L., 2017. Storms, channel changes, and a sediment budget for an urban-suburban stream, Difficult Run, Virginia, USA. Geomorphology 278, 128–148.

Goodwin, T.H., Young, A.R., Holmes, M.G.R., Old, G.H., Hewitt, N., Leeks, G.J.L., Packman, J.C., Smith, B.P.G., 2003. The temporal and spatial variability of sediment transport and yields within the Bradford Beck catchment, West Yorkshire. Science of The Total Environment, Land Ocean Interaction: processes, functioning and environmental management: a UK perspective 314–316, 475–494. https://doi.org/10.1016/S0048-9697(03)00069-X.

Graf, W.L., 1975. The impact of suburbanization on fluvial geomorphology. Water Resour. Res. 11, 690–692. https://doi.org/10.1029/WR011i005p00690.

Gray, J.R., Simões, F.J.M., 2008. Estimating Sediment Discharge. American Society of Civil Engineers, pp. 1067–1088. doi:https://doi.org/10.1061/9780784408148.apd.

Guy, H., 1969. Laboratory Theory And Methods for Sediment Analysis. U.S. Geological Survey Techniques Water-Resources Investigation, Book 5, Chapter C1, 58 p.

Guy, H.P., Ferguson, G.E., 1962. Sediment in small reservoirs due to urbanization. J. Hydraul. Div. 88, 27–37.

Hammer, T.R., 1972. Stream channel enlargement due to urbanization. Water Resour. Res. 8, 1530–1540. https://doi.org/10.1029/WR008i006p01530.

Horowitz, A.J., 2006. The effect of the "Great Flood of 1993" on subsequent suspended sediment concentrations and fluxes in the Mississippi River Basin, USA. Sediment Dynamics and the Hydromorphology of Fluvial Systems (Proceedings of a symposium held in Dundee, UK). IAHS 306.

Horowitz, A.J., 2008. Determining annual suspended sediment and sediment-associated trace element and nutrient fluxes. Sci. Total Environ. 400, 315–343. https://doi.org/10.1016/j.scitotenv.2008.04.022.

Horowitz, A.J., 2009. Monitoring suspended sediments and associated chemical constituents in urban environments: lessons from the city of Atlanta, Georgia, USA Water Quality Monitoring Program. J. Soils Sediments 9, 342–363. https://doi.org/10.1007/s11368-009-0092-y.

Hupp, C.R., Noe, G.B., Schenk, E.R., Benthem, A.J., 2013. Recent and historic sediment dynamics along Difficult Run, a suburban Virginia Piedmont stream. Geomorphology 180–181, 156–169. https://doi.org/10.1016/j.geomorph.2012.10.007.

Knott, J.M., Sholar, C.J., Matthes, W.J., 1992. Quality assurance guidelines for the analyses of sediment concentration by U.S. Geological Survey sediment laboratories (USGS Numbered Series No. 92–33), Open-File Report. U.S. Dept. of the Interior, U.S. Geological Survey: Books and Open-File Reports Section [distributor],

Langlois, J.L., Johnson, D.W., Mehuys, G.R., 2005. Suspended sediment dynamics associated with snowmelt runoff in a small mountain stream of Lake Tahoe (Nevada). Hydrol. Process. 19, 3569–3580. https://doi.org/10.1002/hyp.5844.

Lawler, D.M., Petts, G.E., Foster, I.D.L., Harper, S., 2006. Turbidity dynamics during spring storm events in an urban headwater river system: The Upper Tame, West Midlands, UK. Science of The Total Environment, Urban Environmental Research in the UK: The Urban Regeneration and the Environment (NERC URGENT) Programme and associated studies. 360, 109–126. doi:https://doi.org/10.1016/j.scitotenv.2005.08.032.

Leopold, L.B., 1968. Hydrology for urban land planning - a guidebook on the hydrologic effects of urban land use. Geol. Surv. Circ. 554.

Leopold, L.B., 1973. River channel change with time: an example address as retiring president of the Geological Society of America, Minneapolis, Minnesota, November 1972. GSA Bull. 84, 1845–1860. https://doi.org/10.1130/0016-7606(1973)84<1845:RCCWTA>2.0.CO;2.

Leopold, L.B., Huppman, R., Miller, A., 2005. Geomorphic effects of urbanization in forty-one years of observation. Proc. Am. Philos. Soc. 149, 349–371.

Mather, A.L., Johnson, R.L., 2014. Quantitative characterization of stream turbidity-discharge behavior using event loop shape modeling and power law parameter decorrelation. Water Resour. Res. 50, 7766–7779. https://doi.org/10.1002/2014WR015417.

Meade, R.H., Moody, J.A., 2010. Causes for the decline of suspended-sediment discharge in the Mississippi River system, 1940–2007. Hydrol. Process. 24, 35–49. https://doi.org/10.1002/hyp.7477.

Nelson, E.J., Booth, D.B., 2002. Sediment sources in an urbanizing, mixed land-use watershed. J. Hydrol. 264, 51–68. https://doi.org/10.1016/S0022-1694(02)00059-8.

Nolan, K.M., Gray, J.R., Glysson, G.D., 2005. Introduction to suspended-sediment sampling. U.S. Geological Survey Scientific Investigations Report 2005–5077.

Pizzuto, J.E., Hession, W.C., McBride, M. 2000 Comparing gravel-bed rivers in paired urban and rural catchments of southeastern Pennsylvania. Geology 28, 79–82. doi:10.1130/0091-7613(2000)028<0079:CGRIPU>2.0.CO;2

Porterfield, G., 1972. Computation of Fluvial-Sediment Discharge, Techniques of Water-Resources Investigations of the United States Geological Survey. U.S. Government Printing Office, Washington DC, Book 3. Chapter 3, 66.

Rantz, S.L., et al., 1982a. Measurement and Computation of Streamflow: Volume 1. Measurement of Stage and Discharge. U.S. Geological Survey Water-Supply Paper 2175. U.S. Government Printing Office, Washington DC.

Rantz, S.L., et al., 1982b. Measurement and Computation of Streamflow: Volume 2. Computation of Discharge. U.S. Geological Survey Water-Supply Paper 2175. U.S. Government Printing Office, Washington DC.

Rasmussen, P.P., Gray, J.R., Glysson, G.D., Ziegler, A.C., 2011. Guidelines and Procedures for Computing Time-Series Suspended-Sediment Concentrations and Loads from In-Stream Turbidity-Sensor and Streamflow Data. U.S. Geological Survey Techniques and Methods Book 3. Chapter 4, 53.

Russell, K.L., Vietz, G.J., Fletcher, T.D., 2017. Global sediment yields from urban an urbanizing watersheds. Earth Sci. Rev. 168, 73–80. https://doi.org/10.1016/j.earscirev.2017.04.001.

Sauer, V.B., 2002. Standards for the analysis and processing of surface-water data and information using electronic methods. U.S. Geol. Surv. Water Resour. Invest. Rep. 01-4044, 91.

Shreve, E.A., Downs, A.C., 2005. Quality-assurance plan for the analysis of fluvial sediment by the U.S. Geological Survey Kentucky Water Science Center Sediment Laboratory. U.S. Geol. Surv. Open File Rep. 2005-1230, 28.

Smith, H.G., Dragovich, D., 2009. Interpreting sediment delivery processes using suspended sediment-discharge hysteresis patterns from nested upland catchments, south-eastern Australia. Hydrol. Process. 23, 2415–2426. https://doi.org/10.1002/hyp.7357.

Taylor, K.G., Owens, P.N., 2009. Sediments in urban river basins: a review of sediment–contaminant dynamics in an environmental system conditioned by human activities. J. Soils Sediments 9, 281–303. https://doi.org/10.1007/s11368-009-0103-z.

Trimble, S.W., 1997. Contribution of stream channel erosion to sediment yield from an urbanizing watershed. Science 278, 1442–1444. https://doi.org/10.1126/science.278.5342.1442.

Walling, D., Webb, B., 1982. Sediment availability and the prediction of storm-period sediment yields. Recent Developments in the Explanation and Prediction of Erosion and Sediment Yield (Proceedings of the Exeter Symposium, July 1982). IAHS Publ. 137.

Walsh, C.J., Roy, A.H., Feminella, J.W., Cottingham, P.D., Groffman, P.M., Morgan, R.P., 2005. The urban stream syndrome: current knowledge and the search for a cure. J. N. Am. Benthol. Soc. 24, 706–723. https://doi.org/10.1899/04-028.1.

Wolman, M.G., 1967. A cycle of sedimentation and erosion in urban river channels. Geogr. Ann. Ser. B 49, 385–395. https://doi.org/10.2307/520904.

Wolman, M.G., Schick, A.P., 1967. Effects of construction on fluvial sediment, urban and suburban areas of Maryland. Water Resour. Res. 3, 451–464. https://doi.org/10.1029/WR003i002p00451.

Yeshaneh, E., Eder, A., Blöschl, G., 2014. Temporal variation of suspended sediment transport in the Koga catchment, North Western Ethiopia and environmental implications. Hydrol. Process. 28, 5972–5984. https://doi.org/10.1002/hyp.10090.

Yorke, T.H., Herb, W.J., 1978. Effects of urbanization on streamflow and sediment transport in the Rock Creek and Anacostia River basins, Montgomery County, Maryland, 1962-74. U.S. Geol. Surv. Prof. Pap. 1003, 63.

Zeiger, S.J., Hubbart, J.A., 2016. Nested-scale nutrient flux in a mixed-land-use urbanizing watershed. Hydrol. Process. 30, 1475–1490.